2009 American Control Conference
Hyatt Regency Riverfront, St. Louis, MO, USA
June 10-12, 2009

Linear Quadratic Optimal Control of Contact Transition with Fingertip

Weiwei Li and Francisco Valero-Cuevas

Abstract— **This paper proposes an optimal control methodology that addresses the problem of control of fingertip during a general class of task that requires the fingertip to make a transition from non-contact motion to contact motion. Specifically, the task that the fingertip makes and transitions from motion to static well-directed force production. Here we present a mathematical framework for controlling the contact transition, while switching between non-contact and contact controller is needed and handled by the optimal control strategy. The non-linear differential algebraic equation that describes the dynamics of the index finger is linearized, and then a modified linear quadratic optimal control problem is solved. The resulting optimal feedback control law guarantees good regulation of contact force, velocity and position. Simulation results are presented to demonstrate the effectiveness of the new approach.**

I. Introduction

Contact transition in dextrous robotic manipulators is a very challenging control problem, because it involves the well-known characteristics of discontinuous nonlinear dynamics, between an open and a closed-loop kinematic chain. The nonzero approaching velocity results in the instability [3], [5] and undesirably high impact force. Furthermore, the unknown nonlinear relationship of the reaction force and deformation is another difficulty for transition control from free to constrained motion.

During the last three decades, researchers in the control engineering and robotics have been putting lots of effort into applying robotic manipulators to contact tasks [2], [6], [10], [20]. Based on the recognition that the controller changes the dynamic behavior of the system, Hogan [3] proposed the use of impedance control approach to achieve stable control of the force exerted on a rigid surface. By using this implementation, both free motions and contact tasks can be controlled successfully using one single control algorithm, and the control is achieved without the difficult inverse kinematic computations. The control solution that Mills *et al.* [9] proposed was the combination of two separate controls: one for non-contact motion and another for contact motion. By utilizing the generalized dynamical system (GDS) theory, they developed an asymptotically stable discontinuous control approach to deal with the contact instability problems. Hyde and co-workers [1], [4] developed an input command preshaping method that suppressed the end-effector vibration by modifying feedforward information during contact transition. However, the problem with the above algorithms, such as the impedance control, the input command shaping, and the discontinuous control, is that they all require the environment dynamics to be accurately modelled (i.e. a linear dumped spring or the stiffness and surface location of the environment) and integrated into controller design. For dealing with uncertainties in different task environments, another group of researchers studied the impact control and force regulation using positive acceleration feedback together with an event-driven switching control strategy. By introducing the nonlinear feedback control law, the dynamic model is feedback-linearized and decoupled [11], [12], [13], [19]. The peak impact force and bouncing can be controlled, the stable contact transition can be achieved and the desired output force can be regulated in an unknown environment without readjusting the gains.

Although there are many successful applications of practical dextrous manipulators in industry, such as assembly tasks for automated manufacturing, robotic gripping, and interactive robot for service tasks, the ability for robots to perform dextrous tasks as humans remains a fascination. Fine manipulation is a distinctive feature of human motor behavior, hence biological systems themselves should provide meaningful solution for the study of contact transition control. Recently, experimental findings on human finger contact transition [17], [18] demonstrated that the muscle coordination pattern [15], [16] clearly switched from motion to well-directed isometric force production before contact. They further proposed that the underlying neural control of finger musculature was predictive and also switched in a time-critical manner from controlling finger motion to controlling fingertip force. In the study of motor control, Todorov *et al.* [8], [14] has pointed out, the sensorimotor system is the product of optimization processes (i.e. evolution, development, learning, adaptation) which continuously improve behavioral performance. Optimality hence provides an elegant framework for trying to explain why the system behaves as it does, and to specify the control laws that generate the observed behavior. Does the control scheme used by the biological system for contact transitions approach a strategy that is optimal or suboptimal?

This paper focuses on the study of the human finger movement and develops a new algorithm for transition control from finger motion to static fingertip force production. The new method is based on the linear quadratic optimal control theory. The aim of this research is to achieve smooth, stable

This work is supported by the National Institutes of Health Grant.

Weiwei Li is with Department of Biomedical Engineering, University of Southern California, Los Angeles, CA 90089 weiweili@usc.edu

Francisco Valero-Cuevas is with Faculty of Department of Biomedical Engineering, and Division of Biokinesiology and Physical Therapy, University of Southern California, Los Angeles, CA 90089 valero@usc.edu

transitions and to avoid instability and large impact force spikes during the controller switching, while increasing the applied force from zero to the desired level as rapidly as possible. We shall show that stable contact transition and desired force regulation can be achieved by the resulting feedback control law. The simulation results clearly demonstrate the effectiveness and advantages of the proposed approach.

The paper is organized as follows. In section II the dynamical models for unconstrained and constrained motion are formulated. The design of the optimal feedback controller for contact transition is developed in section III and an algorithm for the control design is derived which guarantees the performance requirement. Section IV presents a numerical example, and concluding remarks are drawn in section V.

II. System Model and Problem Formulation

A. Open chain dynamics model for unconstrained motion

Consider an index finger model [15] with n joints moving in the horizontal plane. The inverse dynamics is

$$\mathcal{M}(\theta)\ddot{\theta} + \mathcal{C}(\theta,\dot{\theta}) + \mathcal{G}(\theta) = \tau, \tag{1}$$

where $\theta \in \mathbf{R}^n$ is the joint angle vector, $\mathcal{M}(\theta) \in \mathbf{R}^{n\times n}$ is a positive definite symmetric inertia matrix, $\mathcal{C}(\theta,\dot{\theta}) \in \mathbf{R}^n$ is a vector centripetal and Coriolis forces, $\mathcal{G} \in \mathbf{R}^n$ is the gravity force, and $\tau \in \mathbf{R}^n$ is the joint torque. Here we consider direct torque control (i.e. τ is the control signal).

B. Closed chain dynamics model for constrained motion

Let $p \in \mathbf{R}^n$ denote the position vector of the fingertip in the Cartesian coordinate system, then the relation between the Cartesian and the joint coordinate system can be expressed as $p = H(\theta)$, and the Jacobian matrix is defined as

$$J(\theta) = \frac{\partial H(\theta)}{\partial \theta}. \tag{2}$$

Suppose the constraints are such that the position vector of the fingertip satisfies the following algebraic function

$$\Phi(p) = 0, \tag{3}$$

where $\Phi : \mathbf{R}^n \to \mathbf{R}^m$ is the constraint function and $m < n$.

The resulting equations of motion for the non-slipping finger where the fingertip makes contact with the constraint surface are represented as

$$\mathcal{M}(\theta)\ddot{\theta} + \mathcal{C}(\theta,\dot{\theta}) + \mathcal{G}(\theta) + J(\theta)^T f = \tau_c, \tag{4}$$

The contact force f between the fingertip and the constraint surface can be calculated as follows using Lagrange multipliers and Jacobian matrix of the constraint vector function Φ for the fingertip

$$f = \left(\frac{\partial \Phi}{\partial p}\right)^T \lambda, \tag{5}$$

where $\lambda \in \mathbf{R}^m$ is a vector of generalized multipliers associated with the constraints. Hence the differential algebraic equations (3)-(5) define the dynamic model of finger, constrained by contact with a rigid environment.

III. Optimal Controller Design for Contact Transition

The dynamic model is different during free and constrained motion. In the following, an optimal control problem for regulation of contact force and position in free and constrained systems is considered.

A. LQ controller for unconstrained motion

Here we develop the control law of finger during free motion using iterative linear quadratic regulator method. This method uses iterative linearization of the nonlinear system around a nominal trajectory, and computes a locally optimal feedback control law via a modified LQR technique. The control law is then applied to the linearized system, and the result is used to improve the nominal trajectory incrementally.

Based on equations (1), we can compute the forward dynamics and write the system into a form

$$\dot{x} = F(x,u), \tag{6}$$

where the state $x = [\theta;\ \dot{\theta}] \in \mathbf{R}^{2n}$, and control $u = \tau \in \mathbf{R}^n$. The objective of optimal control is to find the control law that minimizes

$$\mathcal{V} = \frac{1}{2}(x(t_f)-x^*)^T Q_f (x(t_f)-x^*) + \frac{1}{2}\int_0^{t_f} \left(x^T Q x + u^T R u\right) dt \tag{7}$$

where Q_f and $Q \in \mathbf{R}^{2n\times 2n}$ are symmetric and positive semi-definite, $R \in \mathbf{R}^{n\times n}$ is symmetric and positive definite.

The locally-optimal control law is constructed iteratively. Each iteration starts with a nominal control sequence u_k, and a corresponding nominal trajectory x_k obtained by applying u_k to the dynamical system (6) in open loop. The linearized discrete dynamics is expressed in terms of the deviations

$$\delta x_{k+1} = A_k \delta x_k + B_k \delta u_k, \tag{8}$$

where $A_k = I + \Delta t \frac{\partial F}{\partial x}\big|_{(x_k,u_k)}, B_k = \Delta t \frac{\partial F}{\partial u}\big|_{(x_k,u_k)}, \Delta t = t_f/(N-1)$. Based on the above linearized model, we can solve the following LQR problem with the cost function

$$\begin{aligned}\mathcal{V} &= \frac{1}{2}(x_N + \delta x_N - x^*)^T Q_f\ (x_N + \delta x_N - x^*) \\ &\quad + \frac{1}{2}\sum_{k=0}^{N-1}\Big\{(x_k+\delta x_k)^T Q\ (x_k+\delta x_k) \\ &\quad + (u_k+\delta u_k)^T R\ (u_k+\delta u_k)\Big\}.\end{aligned} \tag{9}$$

Theorem 1: Given the system (6) and its linearization (8) around the nominal trajectory with the performance index given in (9), the optimal controller is given by

$$\delta u_k = -K\delta x_k - K_v v_{k+1} - K_u u_k, \tag{10}$$

$$K = (B_k^T S_{k+1} B_k + R)^{-1} B_k^T S_{k+1} A_k, \tag{11}$$

$$K_v = (B_k^T S_{k+1} B_k + R)^{-1} B_k^T, \tag{12}$$

$$K_u = (B_k^T S_{k+1} B_k + R)^{-1} R, \tag{13}$$

$$S_k = A_k^T S_{k+1}(A_k - B_k K) + Q, \tag{14}$$

$$v_k = (A_k - B_k K)^T v_{k+1} - K^T R u_k + Q x_k \tag{15}$$

with boundary conditions

$$S_N = Q_f, \qquad v_N = Q_f(x_N - x^*). \tag{16}$$

B. LQ controller for constrained motion

The system of constrained dynamics(3)-(4), introduced in section II, can be written by

$$\dot{x} = F(x, u, \lambda), \tag{17}$$

where the state and control are given by $x = [\theta;\ \dot{\theta}] \in \mathbf{R}^{2n}, u = \tau_c \in \mathbf{R}^n$, and the Lagrangian multipliers $\lambda \in \mathbf{R}^m$. The objective of optimal control is to find the control law that minimizes

$$\begin{aligned} \mathcal{V} &= \frac{1}{2}\left(x(t_f) - x^*\right)^T Q_f \left(x(t_f) - x^*\right) \\ &\quad + \frac{1}{2}\int_0^{t_f} \left(x^T Q x + \lambda^T P \lambda + u^T R u\right) dt \end{aligned} \tag{18}$$

where $Q_f, Q \in \mathbf{R}^{2n\times 2n}$ and $P \in \mathbf{R}^{m\times m}$ are symmetric and positive semi-definite, $R \in \mathbf{R}^{n\times n}$ is symmetric and positive definite.

We first present the linearization of the nonlinear differential-algebraic equations (3)-(4) at the constrained equilibrium (x_0, λ_0), where $x_0 = [\theta_0; 0]$ and λ_0 are constant vectors such that $\Phi(H(\theta_0)) = 0$ and rank $\left(\frac{\partial \Phi}{\partial p} J\right)\Big|_{\theta_0} = m$.

Let u_0 be a constant vector such that

$$u_0 = \mathcal{C}(\theta_0, 0) + \mathcal{G}(\theta_0) + \left(\frac{\partial \Phi}{\partial p} J\Big|_{\theta_0}\right)^T \lambda_0.$$

The linearization is defined in terms of $\delta x_k = x_k - x_0$ and $\delta\lambda_k = \lambda_k - \lambda_0$ as

$$\delta x_{k+1} = A\ \delta x_k + B\ \delta u_k + C\ \delta\lambda_k, \tag{19}$$

$$0 = D\ \delta x_k \tag{20}$$

where $\Delta t = t_f/(N-1)$ and

$$A = I + \Delta t \frac{\partial F}{\partial x}\Big|_{(x_0,\lambda_0)}, \quad B = \Delta t \frac{\partial F}{\partial u}\Big|_{(x_0,\lambda_0)},$$

$$C = \Delta t \frac{\partial F}{\partial \lambda}\Big|_{(x_0,\lambda_0)}, \quad D = \Delta t \frac{\partial \Phi}{\partial p} J\Big|_{x_0}.$$

Definition 1 (Control Relative Degree): The constrained systems (19) and (20) are said to have control relative degree r_i for the i^{th} constraint output and the control input δu_k if

(i) $D_i A^j B = 0, \quad 0 \le j \le r_i - 2,\ i = 1, \cdots, m,$

(ii) $D_i A^{r_i - 1} B \neq 0.$

Definition 2 (Constraint Relative Degree): Systems (19) and (20) are said to have constraint relative degree σ_i for the i^{th} constraint output and the constraint input $\delta\lambda_k$ if

(i) $D_i A^j C = 0, \quad 0 \le j \le \sigma_i - 2,\ i = 1, \cdots, m,$

(ii) $D_i A^{\sigma_i - 1} C \neq 0.$

Now the linearized constrained dynamics(19)-(20) can be described by a state space realization using a linear transformation identical to that given in [7]. First we assume that the constraint relative degree σ_i is not greater that the control relative degree r_i for the i^{th} constraint output, then construct the following matrix

$$\Gamma = \left[C^T; D_1; \cdots; D_1 A^{\sigma_1 - 2}; \cdots; D_m; \cdots; D_m A^{\sigma_m - 2}\right]$$

Suppose the singular value decomposition of $\Gamma \in \mathbf{R}^{(\sigma_1+\cdots+\sigma_m)\times n}$ is given by

$$\Gamma = U[\Sigma \quad 0] \begin{bmatrix} V_1^T \\ V_2^T \end{bmatrix},$$

where $\Sigma \in \mathbf{R}^{(\sigma_1+\cdots+\sigma_m)\times(\sigma_1+\cdots+\sigma_m)}$, $V_1 \in \mathbf{R}^{n\times(\sigma_1+\cdots+\sigma_m)}$ and $V_2 \in \mathbf{R}^{n\times(n-(\sigma_1+\cdots+\sigma_m))}$, by constructing the nonsingular matrix

$$T = \begin{bmatrix} D_1 \\ \vdots \\ D_1 A^{\sigma_1 - 1} \\ \vdots \\ D_m \\ \vdots \\ D_m A^{\sigma_m - 1} \\ V_2^T \end{bmatrix}$$

and introducing the following linear transformation

$$\begin{bmatrix} \delta\tilde{x}_k \\ \delta\bar{x}_k \end{bmatrix} = T\ \delta x_k,$$

where $\delta\tilde{x}_k \in \mathbf{R}^{\sigma_1+\cdots+\sigma_m}$ and $\delta\bar{x}_k \in \mathbf{R}^{n-(\sigma_1+\cdots+\sigma_m)}$, we obtain a state space realization

$$\delta\bar{x}_{k+1} = \bar{A}\ \delta\bar{x}_k + \bar{B}\ \delta u_k, \tag{21}$$

$$\delta\lambda_k = \bar{D}\ \delta\bar{x}_k + \bar{E}\ \delta u_k, \tag{22}$$

where

$$\bar{A} = V_2^T A W_2, \qquad \bar{B} = V_2^T B,$$

$$\bar{D} = -G^{-1} H W_2, \qquad \bar{E} = -G^{-1} L,$$

$$G = \begin{bmatrix} D_1 A^{\sigma_1 - 1} C \\ \vdots \\ D_m A^{\sigma_m - 1} C \end{bmatrix}, \qquad H = \begin{bmatrix} D_1 A^{\sigma_1} \\ \vdots \\ D_m A^{\sigma_m} \end{bmatrix},$$

$$L = \begin{bmatrix} D_1 A^{\sigma_1 - 1} B \\ \vdots \\ D_m A^{\sigma_m - 1} B \end{bmatrix}, \qquad T^{-1} = \begin{bmatrix} W_1 & W_2 \end{bmatrix},$$

and $\delta\bar{x}_k = V_2^T \delta x_k, \delta x_k = W_2 \delta\bar{x}_k$.

Applying the above state-space transformation results, the original optimal control problem described by (17)-(18) can be rewritten as

$$\begin{aligned} \mathcal{V} &= \frac{1}{2}(\delta\bar{x}_N - \delta\bar{x}^*)^T \bar{Q}_f\ (\delta\bar{x}_N - \delta\bar{x}^*) \\ &\quad + \frac{1}{2}\sum_{k=0}^{N-1} \Big\{ x_0^T Q x_0 + \lambda_0^T P \lambda_0 + u_0^T R u_0 \\ &\quad + \delta\bar{x}_k^T \bar{x}_0 + \bar{x}_0^T \delta\bar{x}_k + \delta u_k^T \bar{u}_0 + \bar{u}_0^T \delta u_k \\ &\quad + \delta\bar{x}_k^T \bar{Q}\ \delta\bar{x}_k + \delta\bar{x}_k^T \bar{P}\ \delta u_k + \delta u_k^T \bar{P}^T\ \delta\bar{x}_k \\ &\quad + \delta u_k^T \bar{R}\ \delta u_k \Big\}, \end{aligned} \tag{23}$$

where $\bar{u}_0, \bar{x}_0, \bar{Q}, \bar{P}$ and $\bar{R}$ are defined by

$$\bar{u}_0 = Ru_0 + \bar{E}^T P\lambda_0, \quad \bar{x}_0 = W_2^T Q x_0 + \bar{D}^T P\lambda_0,$$
$$\delta\bar{x}^* = V_2^T(x^* - x_0), \quad \bar{Q}_f = W_2^T Q W_2,$$
$$\bar{Q} = W_2^T Q W_2 + \bar{D}^T P\bar{D},\ \bar{P} = \bar{D}^T P\bar{E},\ \bar{R} = R + \bar{E}^T P\bar{E}.$$

Theorem 2: Given the system (17), its linearization (19)-(20) around the constrained equilibrium, and the equivalent state realization (21)-(22) with the performance index given in (23), the optimal controller is given by

$$\delta u_k = -(K + \bar{R}^{-1}\bar{P}^T)\delta\bar{x}_k - K_v v_{k+1} - K_u\bar{u}_0, \tag{24}$$
$$K = (\bar{B}^T S_{k+1}\bar{B} + \bar{R})^{-1}\bar{B}^T S_{k+1}\mathcal{A}, \tag{25}$$
$$K_v = (\bar{B}^T S_{k+1}\bar{B} + \bar{R})^{-1}\bar{B}^T, \tag{26}$$
$$K_u = (\bar{B}^T S_{k+1}\bar{B} + \bar{R})^{-1}, \tag{27}$$
$$S_k = \mathcal{A}^T S_{k+1}(\mathcal{A} - \bar{B}K) + \mathcal{Q}, \tag{28}$$
$$v_k = (\mathcal{A} - \bar{B}K)^T v_{k+1} - (K + \bar{R}^{-1}\bar{P}^T)^T\bar{u}_0 + \bar{x}_0 \tag{29}$$

where

$$\mathcal{A} = \bar{A} - \bar{B}\bar{R}^{-1}\bar{P}^T, \qquad \mathcal{Q} = \bar{Q} - \bar{P}\bar{R}^{-1}\bar{P}^T, \tag{30}$$

with boundary conditions

$$S_N = W_2^T Q_f W_2, \qquad v_N = W_2^T Q_f(x_0 - x^*). \tag{31}$$

Proof: We begin with the Hamiltonian function

$$\begin{aligned} H_k \;=\; & \frac{1}{2}\Big\{ x_0^T Q x_0 + \lambda_0^T P\lambda_0 + u_0^T R u_0 \\ & + \delta\bar{x}_k^T\bar{x}_0 + \bar{x}_0^T\delta\bar{x}_k + \delta u_k^T\bar{u}_0 + \bar{u}_0^T\delta u_k \\ & + \delta\bar{x}_k^T\bar{Q}\,\delta\bar{x}_k + \delta\bar{x}_k^T\bar{P}\,\delta u_k + \delta u_k^T\bar{P}^T\,\delta\bar{x}_k \\ & + \delta u_k^T\bar{R}\,\delta u_k\Big\} + \delta\gamma_{k+1}^T(\bar{A}\delta\bar{x}_k + \bar{B}\delta u_k), \end{aligned}$$

where $\delta\gamma_{k+1}$ is Lagrange multiplier.

The optimal control improvement δu_k is given by solving the state equation (21), the costate equation

$$\delta\gamma_k = \bar{A}^T\delta\gamma_{k+1} + \bar{Q}\delta\bar{x}_k + \bar{P}\delta u_k + \bar{x}_0, \tag{32}$$

and the stationary condition which can be obtained by setting the derivative of Hamiltonian function with respect to δu_k to zero

$$0 = \bar{u}_0 + \bar{P}^T\delta\bar{x}_k + \bar{R}\delta u_k + B_k^T\delta\gamma_{k+1} \tag{33}$$

with the boundary condition

$$\delta\gamma_N = \bar{Q}_f\left(\delta\bar{x}_N - V_2^T(x^* - x_0)\right). \tag{34}$$

Solving for (33) yields

$$\delta u_k = -\bar{R}^{-1}\left[\bar{B}^T\delta\gamma_{k+1} + \bar{P}^T\delta\bar{x}_k + \bar{u}_0\right]. \tag{35}$$

Hence, substituting (35) into (21) and combining it with (32), the resulting Hamiltonian system is

$$\begin{pmatrix} \delta\bar{x}_{k+1} \\ \delta\gamma_k \end{pmatrix} = \begin{pmatrix} \mathcal{A} & -\bar{B}\bar{R}^{-1}\bar{B}^T \\ \mathcal{Q} & \mathcal{A}^T \end{pmatrix}\begin{pmatrix} \delta\bar{x}_k \\ \delta\gamma_{k+1} \end{pmatrix} + \begin{pmatrix} -\bar{B}\bar{R}^{-1}\bar{u}_0 \\ \bar{x}_0 - \bar{P}\bar{R}^{-1}\bar{u}_0 \end{pmatrix}. \tag{36}$$

It is clear that the Hamiltonian system is not homogeneous, but is driven by a forcing term dependent on $\bar{x}_0$ and $\bar{u}_0$. Because of the forcing term, it is not possible to express the optimal control law in linear state feedback form (as in the classic LQR case). However, we can express δu_k as a combination of a linear state feedback plus additional terms, which depend on the forcing function.

Based on the boundary condition (34), we assume

$$\delta\gamma_k = S_k\delta\bar{x}_k + v_k \tag{37}$$

for some unknown sequences S_k and v_k.

In order to find the equations (24)-(29), use (37) in the state equation (21) to yield

$$\begin{aligned} \delta\bar{x}_{k+1} = (I + \bar{B}\bar{R}^{-1}B^T S_{k+1})^{-1}(\mathcal{A}\delta\bar{x}_k \\ - \bar{B}\bar{R}^{-1}\bar{B}^T v_{k+1} - \bar{B}\bar{R}^{-1}\bar{u}_0). \end{aligned} \tag{38}$$

Substituting (37) and the above equation into the costate equation (32) gives

$$\begin{aligned} S_k\delta\bar{x}_k + v_k = \mathcal{Q}\delta\bar{x}_k + \mathcal{A}^T S_{k+1}(I + \bar{B}\bar{R}^{-1}\bar{B}^T S_{k+1})^{-1} \\ (\mathcal{A}\delta\bar{x}_k - \bar{B}\bar{R}^{-1}\bar{B}^T v_{k+1} - \bar{B}\bar{R}^{-1}\bar{u}_0) \\ + \mathcal{A}^T v_{k+1} + \bar{x}_0 - \bar{P}\bar{R}^{-1}\bar{u}_0. \end{aligned}$$

By applying the matrix inversion lemma [1] to the above equation, we obtain

$$S_k = \mathcal{A}^T S_{k+1}\Big[I - \bar{B}(\bar{R} + \bar{B}^T S_{k+1}\bar{B})^{-1}\bar{B}^T S_{k+1}\Big]\mathcal{A} + \mathcal{Q},$$

and

$$\begin{aligned} v_k = {} & \mathcal{A}^T v_{k+1} \\ & - \mathcal{A}^T S_{k+1}\Big[I - \bar{B}(\bar{R} + \bar{B}^T S_{k+1}\bar{B})^{-1}\bar{B}^T S_{k+1}\Big]\bar{B}\bar{R}^{-1}\bar{B}^T v_{k+1} \\ & - \mathcal{A}^T S_{k+1}\Big[I - \bar{B}(\bar{R} + \bar{B}^T S_{k+1}\bar{B})^{-1}\bar{B}^T S_{k+1}\Big]\bar{B}\bar{R}^{-1}\bar{u}_0 \\ & + \bar{x}_0 - \bar{P}\bar{R}^{-1}\bar{u}_0. \end{aligned} \tag{39}$$

By using $(\bar{R} + \bar{B}^T S_{k+1}\bar{B})^{-1} = \bar{R}^{-1} - (\bar{R} + \bar{B}^T S_{k+1}\bar{B})^{-1}\bar{B}^T S_{k+1}\bar{B}\bar{R}^{-1}$, the second term in v_k becomes

$$-\mathcal{A}^T S_{k+1}\bar{B}(\bar{R} + \bar{B}^T S_{k+1}\bar{B})^{-1}\bar{B}^T v_{k+1},$$

while the third term in v_k can also be written as

$$-\mathcal{A}^T S_{k+1}\bar{B}(\bar{R} + \bar{B}^T S_{k+1}\bar{B})^{-1}\bar{u}_0.$$

Therefore, with the definition of K in (25), the above S_k, v_k can be written into the forms as given in (28) and (29).

Furthermore, substituting (37) and (38) into (35) yields

$$\begin{aligned} \delta u_k = {} & -(\bar{R} + \bar{B}^T S_{k+1}\bar{B})^{-1}\bar{B}^T S_{k+1}\mathcal{A}\delta\bar{x}_k - \bar{R}^{-1}\bar{P}^T\delta\bar{x}_k \\ & - (\bar{R} + \bar{B}^T S_{k+1}\bar{B})^{-1}\bar{B}^T v_{k+1} \\ & - (\bar{R} + \bar{B}^T S_{k+1}\bar{B})^{-1}\bar{u}_0. \end{aligned}$$

By the definition of K, K_v and K_u in (25)-(27), we can rewrite above δu_k as the form in (24). ■

With the boundary condition S_N given as the final state weighting matrix in the cost function (23), we can solve for

[1] $(A + BCD)^{-1} = A^{-1} - A^{-1}B(DA^{-1}B + C^{-1})^{-1}DA^{-1}$.

an entire sequence of S_k by the backward recursion (28). It is interesting to note that the control law δu_k consists of three terms: a term linear in $\delta\bar{x}_k$ whose gain is dependent on the solution to the Riccati equation; a second term dependent on an auxiliary sequence v_k which is derived from the auxiliary difference equation (29); and a third term dependent on the nominal control $\bar{u}_0$ whose gain also relies on the Riccati equation solution.

IV. Numerical Example

In order to determine the applicability of the method, an example to solve for the control design of contact transition is presented next. Consider an index finger model [15] with 3 joints (metacarpophalangeal (MCP) joint, proximal interphalangeal (PIP) joint, and distal interphalangeal (DIP) joint), moving in the horizontal plane (Fig. 1). The inverse dynamics is described by (1) where the expressions of the different variables and parameters $\mathcal{M}(\theta) \in R^{3\times 3}$, $\mathcal{C}(\theta,\dot{\theta}) \in R^3$ are given by

$$\mathcal{M}_{11} = \mathcal{M}_{31} + a_1 + a_2 + 2a_4 cos\theta_2 \tag{40}$$
$$\mathcal{M}_{21} = \mathcal{M}_{22} + a_4 cos\theta_2 + a_6 cos(\theta_2+\theta_3) \tag{41}$$
$$\mathcal{M}_{22} = \mathcal{M}_{33} + a_2 + 2a_5 cos\theta_3 \tag{42}$$
$$\mathcal{M}_{31} = \mathcal{M}_{32} + a_6 cos(\theta_2+\theta_3) \tag{43}$$
$$\mathcal{M}_{32} = \mathcal{M}_{33} + a_5 cos\theta_3 \tag{44}$$
$$\mathcal{M}_{33} = a_3 \tag{45}$$
$$\begin{aligned}\mathcal{C}_1 = {} & a_4 sin\theta_2 \left[-\dot{\theta}_2(2\dot{\theta}_1+\dot{\theta}_2)\right] \\ & + a_5 sin\theta_3 \left[-\dot{\theta}_3(2\dot{\theta}_1+2\dot{\theta}_2+\dot{\theta}_3)\right] \\ & + a_6 sin(\theta_2+\theta_3)\left[-(\dot{\theta}_2+\dot{\theta}_3)(2\dot{\theta}_1+\dot{\theta}_2+\dot{\theta}_3)\right],\end{aligned} \tag{46}$$
$$\begin{aligned}\mathcal{C}_2 = {} & a_4 sin\theta_2 \dot{\theta_1}^2 + a_5 sin\theta_3 \left[-\dot{\theta}_3(2\dot{\theta}_1+2\dot{\theta}_2+\dot{\theta}_3)\right] \\ & + a_6 sin(\theta_2+\theta_3)\dot{\theta_1}^2,\end{aligned} \tag{47}$$
$$\mathcal{C}_3 = a_5 sin\theta_3 \left(\dot{\theta}_1+\dot{\theta}_2\right)^2 + a_6 sin(\theta_2+\theta_3)\dot{\theta_1}^2, \tag{48}$$
$$a_1 = (m_1+m_2+m_3)l_1^2, \quad a_2 = (m_2+m_3)l_2^2, \tag{49}$$
$$a_3 = m_3 l_3^2, \qquad a_4 = (m_2+m_3)l_1 l_2, \tag{50}$$
$$a_5 = m_3 l_2 l_3, \qquad a_6 = m_3 l_1 l_3, \tag{51}$$

where m_i is the mass for link i ($0.05kg$, $0.05kg$, $0.03kg$), l_i is the length of link i ($6cm$, $6cm$, $5cm$).

The fingertip is constrained to make contact with the rigid constraint surface shown in Fig. 1, so that the constrained dynamic equations are given by (4)-(5), and the constraint condition is

$$\Phi(p) = l_1 cos\theta_1 + l_2 cos(\theta_1+\theta_2) + l_3 cos(\theta_1+\theta_2+\theta_3) = 0. \tag{52}$$

The nonlinear differential-algebraic equations (4)-(5) are linearized about an equilibrium (x_0, λ_0) given by $x_0 = [\frac{\pi}{3}; \frac{\pi}{6}; \frac{37\times\pi}{180}; 0; 0; 0], \lambda_0 = 0.1$.

The task here is to produce a downward tapping motion followed by vertical fingertip force against a rigid surface.

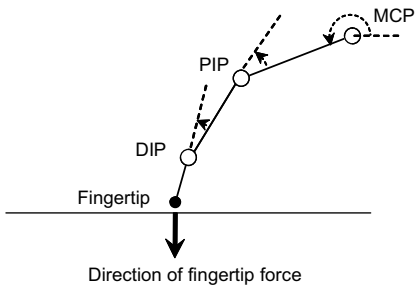

Fig. 1. 3-link index finger with metacarpophalangeal (θ_1: MCP), proximal interphalangeal (θ_2: PIP), and distal interphalangeal (θ_3: DIP) joint

Resembling the experimental data [17], we specify the fingertip to start at rest position at $t = 0ms$, located vertically above the target. During the interval $[0ms; 500ms]$, the fingertip moves downwards and exactly reaches the surface at $t = 500ms$; while during the interval $[500ms; 600ms]$, the fingertip will produce the vertical desired force on the surface.

The cost function is defined by

$$V_{free} = \frac{1}{2}(x(0.5)-x^*)^T(x(0.5)-x^*) + \frac{1}{2}\int_0^{0.5} r\tau^T\tau\, dt, \tag{53}$$

$$\begin{aligned}V_{const} = {} & \frac{1}{2}(x(0.6)-x^*)^T(x(0.6)-x^*) \\ & + \frac{1}{2}\int_{0.5}^{0.6}(r_1\lambda^T\lambda + r_2\tau^T\tau)\, dt,\end{aligned} \tag{54}$$

where the state and control are given by

$$x = (\theta_1\ \theta_2\ \ \theta_3\ \dot{\theta}_1\ \dot{\theta}_2, \dot{\theta}_3)^T, \qquad u = \tau = (\tau_1\ \tau_2\ \tau_3)^T,$$

x^* is the desired target position, $r = 10^{-4}$, $r_1 = 10^{-3}$, and $r_2 = 10^{-4}$ are weighting coefficients. In the definition of the cost function (53), the first term means that the joint angle is going to the target x^* which represents the reaching movement; the second term illustrates the energy efficiency.

The optimal controller for free motion is obtained by minimizing the performance criterion (53) subject to the dynamical system (1), and the control law for constrained motion is obtained by minimizing the cost function (54) subject to the constrained dynamics (4)-(5) and (52). The controller is switched from free to constrained motion at about $350ms$, which is before the contact.

The performance of the contact transition control approach introduced in this paper is illustrated in Fig. 2 and Fig. 3, where the movement trajectories and control commands are plotted. The simulation results show that good regulation of force and position is achieved: the metacarpophalangeal (MCP) joint angle, the proximal interphalangeal (PIP) and the distal interphalangeal (DIP) joint angle arrive to the desired posture $\theta_1 = 60^\circ, \theta_2 = 30^\circ, \theta_3 = 37^\circ$ respectively, and λ arrives to the desired magnitude 0.1 (Fig. 4).

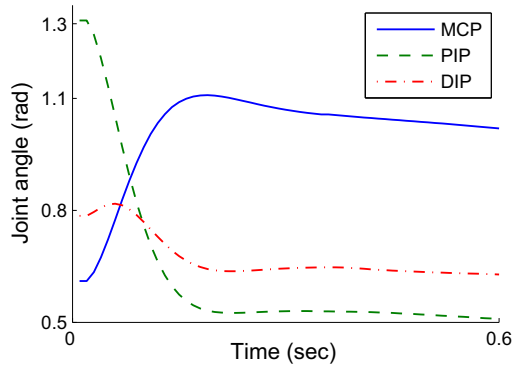

Fig. 2. Optimal trajectories of 3-link index finger joint angles. Blue solid (θ_1:MCP), green dash (θ_2:PIP), and red dashdot (θ_3:DIP)

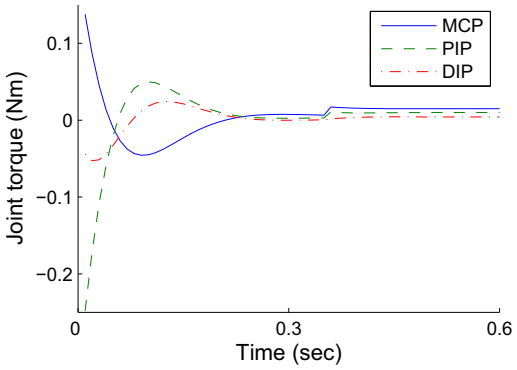

Fig. 3. Optimal joint torques (control command) for 3-link index finger, the joint torque needed for the desired force production switches before the contact

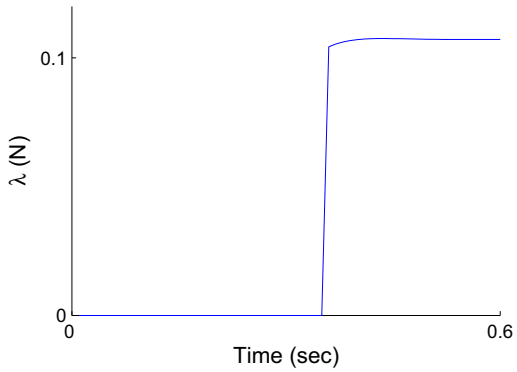

Fig. 4. Force production

V. Conclusions

Optimal control plays a very important role in the study of bio-mechanical movement system. Here we formulate the control of fingertip during contact transition as a linear quadratic optimal control problem. A locally optimal feedback control law is computed for the motion of unconstrained dynamics via a modified LQR technique. The nonlinear differential-algebraic equations which describe the motion of constrained dynamics are linearized about a constrained equilibrium, and then a modified linear quadratic optimal control problem associated with the state space realization of the resulting linear differential-algebraic equations is solved. The simulation results demonstrate that the controller design approach presented in this paper provides good regulation of contact force and position in the transition control of fingertip.

VI. Acknowledgments

The authors gratefully acknowledge the contribution of National Institutes of Health.

References

[1] P.N. Akella and M.R. Cutkosky. Contact transition control with semi-active soft fingertips. *IEEE Transactions on Robotics and Automation* 11, 859-867, 1995.

[2] Z. Doulgeri and Y. Karayiannidis. Force position control for a robot finger with a soft tip and kinematic uncertainties. *Robotics and Autonomous Systems* 55, 328336, 2007.

[3] N. Hogan. On the stability of manipulators performing contact tasks. *IEEE Journal of Robotics and Automation*, 4(6), December 1988.

[4] J.M. Hyde and M.R. Cutkosky. Controlling contact transition. *IEEE Control Systems* 14, 25-30, 1994.

[5] H. Kazerooni. Contact instability of the direct drive robot when constrained by a rigid environment. *IEEE Transactions on Automatic Control* 35, 710-714, 1990.

[6] O. Khatib. A unified approach for motion and force control of robot manipulators: the operational space formulation. *IEEE Journal of Robotics and Automation*, vol. RA-3, no. 1, 43-57, 1987.

[7] H. Krishnan and N.H. McClamroch. On control systems described by a class of linear differential-algebric equations: state realizations and linear quadratic optimal control. *Proceedings of the 1990 American Control Conference*, 818-823, 1990.

[8] W. Li and E. Todorov. Iterative linearization methods for approximately optimal control and estimation of nonlinear stochastic system. *International Journal of Control*, 80(9), 1439-1453, 2007.

[9] J.K. Mills and D.M. Lokhorst. Control of robotic manipulators during general task execution: a discontinuous control approach. *The International Journal of Robotics Research*, 12, 146-163, 1993.

[10] M.H. Raibert and J. J. Craig. Hybrid Position / Force Control of Manipulators. *ASME Journal of Dynamic Systems, Measurment, and Control*, 102, 126-133, 1981.

[11] N. Sarkar, X.P. Yun and R. Ellis. Live-constraint-based control for contact transitions. *IEEE Transactions on Robotics and Automation* 14, 743-754, October 1998.

[12] M. Spong. On the force control problem for flexible joint manipulators. *IEEE Transactions on Automatic Control* 34, 107-111, January 1989.

[13] T.J. Tarn, Y. Wu, N. Xi, and A. Isidori. Force regulation and contact transition control. *IEEE Control Systems*, 32-40, 1996.

[14] E. Todorov and M. Jordan. Optimal feedback control as a theory of motor coordination. *Nature Neuroscience*, 5(11), 1226-1235, 2002.

[15] F.J. Valero-Cuevas. An integrative approach to the biomechanical function and neuromuscular control of the fingers. *Journal of Biomechanics*, 38, 673-684, 2005.

[16] F.J. Valero-Cuevas. A mathematical approach to the mechanical capabilities of limbs and fingers. *Progress in Motor Control V — A Multidisciplinary Perspective*, 615-629, Springer, New York, 2006.

[17] M. Venkadesan and F.J. Valero-Cuevas. Neural control of motion-to-Force transitions with the fingertip. *The Journal of Neuroscience*, 28(6), 1366-1373, February 2008.

[18] M. Venkadesan and F.J. Valero-Cuevas. Effects of neuromuscular lags on controlling contact transitions. *Philosophical Transactions of the Royal Society A*, 367(1891), 1163-1179, March 2009.

[19] D.W. Wang and N.H. McClamroch. Position and force control for constrained manipulator motion: Lyapunov's direct method. *IEEE Transactions on Robotics and Automation*, 9(3), 308-313, 1993.

[20] D. Whitney. Historical perspective and state of the art in robot force control. *The International Journal of Robotics Research*, 6(1), 3-14, 1987.